JOURNAL OF MATERIALS SCIENCE 26 (1991) 2273–2286

Microdeformation and network structure in epoxies

M. D. GLAD*, E. J. KRAMER
Department of Materials Science and Engineering and the Materials Science Center, Cornell University, Ithaca, New York 14853, USA

Thin films of epoxies with various strand densities, ν, are strained in tension until localized plastic deformation is observed. The total strand density, a sum of entanglement and cross-linked strand densities, is adjusted by changing the initial resin molecular weight, the weight fraction of added diluent, and the stoichiometric fraction of curing agent. Experiments on uncrosslinked high molecular weight phenoxy are used to investigate the entanglement network. The strand density ν is computed from measurements of the rubbery plateau modulus using the theory of rubber elasticity and is used to compute the maximum extension ratio of a single network strand, λ_{max}, which varies approximately as $\nu^{-1/2}$. Transmission electron microscopy is used to quantitatively characterize the plastic deformation. Only plane stress deformation zones (DZs) are observed in the cross-linked epoxies, and the entangled phenoxy resins. The characteristic extension ratio in these DZs, λ, is found to scale as $\lambda - 1 = 0.32(\lambda_{max} - 1)$, a relation close to that observed for thermoplastics and cross-linked polystyrene. Rather than promoting a transition from shear deformation to crazing, diluting these networks with unreactive epoxy molecules too short to entangle makes them prone to fracture.

1. Introduction

The fracture of cross-linked polymer glasses, such as epoxies, is the subject of significant controversy. One extreme point of view held strongly in certain quarters [1] is that epoxies are truly brittle materials, that is, incapable of any localized plastic deformation even at the crack tip. Others [2–4] contend that epoxies are prone to crazing, a local mechanism of plastic cavitation which causes other glassy polymers such as polystyrene to fail in a macroscopically brittle manner. Still others [5–8] report that a plastic deformation zone exists ahead of the crack tip in epoxies, but that it is a zone of shear deformation rather than crazing. Whether epoxies deform plastically by crazing or by shear deformation, or deform only elastically has important implications for strategies for toughening this important class of materials. It dictates, for example, the optimum morphology and microstructure of rubber particles in a rubber toughened epoxy [9].

Recent experiments on the thermoplastics [10–14] and radiation cross-linked polystyrene [15] have revealed that the entanglement network, in the former, and the cross-linked network, in the latter, play an important role in determining the deformation mode of the polymer glass. Glassy polymers with a low density of network strands will craze, those with a higher density of network strands will deform by shear, while those with extremely high strand densities will deform predominantly elastically. The deformation mode of an epoxy may depend on its strand density and since a wide range of strand densities is possible in epoxies, the observations reported in the literature may be reconcilable.

We report here the first set of measurements on the microdeformation of thin films of epoxies having a wide range of strand densities, achieved by increasing the starting molecular weight of the epoxy resin, by diluting the network with short non-reactive resin molecules, and by decreasing the amount of cross-linking agent added. The results show conclusively that crazing is not a mechanism of microdeformation in conventional epoxies. The dominant mode of deformation at the crack tip is shear deformation; substantial, but diffuse, shear strains are observed even in the most tightly cross-linked epoxies. Moreover, these results are entirely in agreement with the predictions based on the molecular network approach.

2. Molecular networks

The effect of the underlying microscopic structure of a glassy thermoplastic on its plastic deformation in thin films has been studied extensively [10–15]. This structure has its basis in the interpenetration of the coiled polymer chains and can be characterized by the number density of entanglements that form between the polymer molecules as a result of their interpenetration. The density of entangled strands, ν_E, where a strand is any length of polymer chain bounded by two entanglements, is related to the entanglement molecu-

* *Present address*: Bldg 230-1E-04, 3M Center, St. Paul, Minnesota 55144, USA.

0022–2461/91 $03.00 + .12

lar weight, M_E, by

$$\nu_E = \rho N_A / M_E \quad (1)$$

where ρ is the density of the polymer and N_A is Avogadro's number. The entanglement network may also be characterized by the average contour length of an entangled strand, l_E, given by

$$l_E = (l_0/M_0)M_E \quad (2)$$

where l_0 is the contour length and M_0 the molecular weight of a single repeat unit of the polymer molecule.

In order to relate the entanglement network to the plastic deformation which occurs in these glasses, λ_{max}, the maximum extension ratio of a single strand embedded in the network, is defined to be

$$\lambda_{max} \equiv l_E/d \quad (3)$$

where $d = |\mathbf{d}|$, $\mathbf{d}$ is the vector between the endpoints of the strand, and where it is assumed that no disentanglement or chain scission occurs during deformation. Obviously, d also called the entanglement or network mesh size, is not independent of the other parameters which may be used to characterize the entanglement network. For sufficiently large M_E,

$$d^2 = k^2 M_E \quad (4)$$

where k is a constant which can be determined directly from measurements of molecular dimensions using small angle neutron scattering of the bulk polymer or light scattering of a theta solution containing the polymer, or indirectly from viscosity measurements on dilute solutions. If M_E is not sufficiently large, an alternative relationship derived by Porod and Kratky [16, 17] for a freely jointed worm-like chain must be used in order to relate d to the previously defined network parameters. It is most convenient to express this relationship in terms of l_E and the persistence length, a, of the polymer chain, namely

$$d^2 = 2al_E\{1 - (a/l_E)[1 - \exp(-l_E/a)]\} \quad (5)$$

Note that Equation 5 reduces to Equation 4 when $l_E \gg a$, in which case the persistence length will be given by

$$a = k^2 M_0/2l_0 \quad (6)$$

This formulation assumes that the polymer is a glassy thermoplastic containing no cross-links, where the only topological constraints on the movement of a strand are entanglements. Experiments have also been done on cross-linked PS, however, where there can be an appreciable number of cross-linked strands [15]. In this case, the total strand density used to characterize the network, ν, was just the sum of the entanglement density and the crosslinked strand density, ν_X, i.e.,

$$\nu = \nu_E + \nu_X \quad (7)$$

This equation can be rewritten, using Equations 1 and 2, as,

$$1/l = 1/l_E + 1/l_X \quad (8)$$

The network characterization for the cross-linked system is identical to that for the entangled system with the appropriate substitutions made for the entanglement network parameters.

The plastic zones formed in thin films (0.3 to 1.0 μm) of glassy polymers are either DZs or crazes [10–15]. The crazes, and most of the DZs, have a local extension ratio, λ, which rises sharply in the region bordering the plastic zone and then remains relatively constant across the zone to the opposite border. This constant value of λ can be used to characterize the deformation occurring in these plastic deformation zones. Since different glassy polymers have different intrinsic values for ν_E, it is possible to determine the effects of network structure on plastic deformation by measuring λ in a series of glassy thermoplastics. This determination is also possible by measuring the characteristic λ of PS–PPO blends and of cross-linked PS. In the blends, if the molecular weights of the PS and PPO are both greater than their respective entanglement molecular weights, the strand density of the blend varies between that of the two homopolymers. On the other hand, if the molecular weight of the PS is smaller than its M_E, the PS molecules will not entangle, in effect diluting the entanglement network of the PPO (and decreasing the overall strand density). In the cross-linked PS, the strand density will be increased by increasing the degree of cross-linking.

The results of the measurements of λ in all of these polymers were summarized by Henkee and Kramer [15], who observed a transition from crazing to shear deformation as the strand density was increased [14, 15]. For all the polymers tested, if $\nu < 4 \times 10^{25}\ m^{-3}$, only crazing was observed, but if $\nu > 8 \times 10^{25}\ m^{-3}$, only shear deformation was observed. In the intermediate region where $4 \times 10^{25}\ m^{-3} < \nu < 8 \times 10^{25}\ m^{-3}$, crazes and DZs were observed in competition with one another.

The tendency for a glassy polymer to deform via shear as its strand density is increased results from the additional energy required for chain scission that is necessary to create the fibril surface in a craze. This fibril surface energy, Γ, is approximately [18, 19]

$$\Gamma = \gamma + \tfrac{1}{4} U \nu d \quad (9)$$

where U is the scission energy of a single bond and γ the van der Waals surface energy. Since νd increases as $\nu^{1/2}$, increasing the strand density increases the energy necessary for craze fibril surface formation. By using this treatment, one ought to be able to predict *a priori* which kind of deformation a glassy polymer will exhibit from a knowledge only of its strand density. The strand density of a typical crosslinked epoxy can be estimated to be $150 \times 10^{25}\ m^{-3}$, which from the results of Henkee and Kramer, suggests that it will deform solely by shear deformation [15]. Yet such epoxies are reported by some workers [2] to craze.

The other important feature one may observe in results of Henkee and Kramer is the dependence of the extension ratio on the network structure as characterized by the strand density. This dependence is more

clearly written as

$$(\lambda - 1) \simeq 0.80(\lambda_{max} - 1) \quad (10)$$

for crazes and

$$(\lambda - 1) \simeq 0.40(\lambda_{max} - 1) \quad (11)$$

for DZs [15].

It is the purpose of the present work to see if the above ideas relating the network structure of a polymer glass to its plane stress plastic deformation extend to thermosets. Epoxies are excellent materials for this purpose. In addition to their technological importance, epoxies have a crosslink density which may be easily varied. Since the curing reaction between epoxies and certain primary amines occurs predominantly through the epoxide groups at the ends of the molecule [20, 21], increasing the starting molecular weight of the epoxy resin will increase the distance between crosslinks and, hence, decrease the network strand density. The strand density can also be reduced by diluting the network with short uncrosslinked chains, in analogy to the previous experiments on PPO–PS blends [12]. A third method of reducing the strand density is to decrease the amount of curing agent in the sample from its stoichiometric amount, thereby reducing the number of available crosslink sites in the system.

Since the plastic deformation which occurs at the crack tip in epoxies is largely responsible for their fracture toughness [5, 8, 9, 22] reducing the strand density may also influence this critical property.

3. Experimental procedure

The epoxy resin used in this study was diglycidyl ether of bisphenol A (DGEBA). It has the following structure and was provided by Dow Chemical Co.

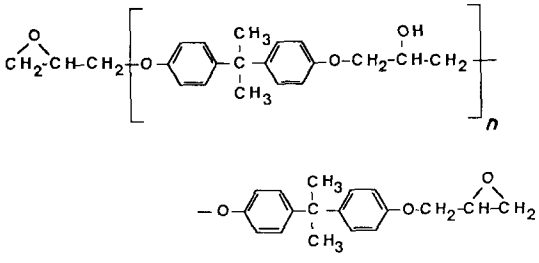

DGEBA

DGEBAs with molecular weights of approximately 350, 500, 1050, 1850, 3600, 40 000, and 70 000 were investigated. The DGEBA resins themselves will be designated by their starting molecular weight, M_R. The term epoxy will be reserved for the final crosslinked epoxy containing one of these resins and may also be designated by M_R. The curing agents used were diethylene triamine (DETA), tetraethylene pentamine (TEPA), methylene dianiline (MDA), and metaphenylene diamine (MPDA). These have the following structures:

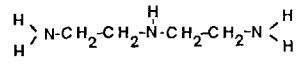

DETA

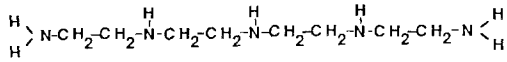

TEPA

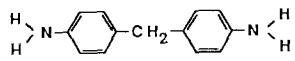

MDA

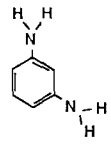

MPDA

Solutions were made by dissolving one epoxy resin and one curing agent in a suitable solvent. Unless otherwise stated the stoichiometric amount of curing agent was added to each solution. This amount was calculated by assuming that each amine hydrogen of the curing agent reacts with one epoxide group of the DGEBA resin, and that no other side reactions occur. The two phenoxy resins with the highest molecular weights require no curing agent and were used to characterize the entanglement network of these epoxies.

The viscosity of each solution was adjusted by adding solvent to allow a film approximately 0.9 μm thick to be spun on to a NaCl substrate. The films of M_R = 70k DGEBA were made by drawing a glass slide at a constant rate from solution. After drying (in air overnight and in a vacuum dessicator for 6 h) the films containing curing agent were subjected to a B-stage cure. This precure varied depending on the curing agent and the molecular weight of the epoxy resin in each of the films. The films containing M_R = 3600 DGEBA and an aliphatic curing agent were precured for 1 h at 100 °C. The remaining films with an aliphatic curing agent were not precured. The films containing MDA and MPDA were precured for 1 h at 100 °C, 1.5 h at 130 °C, and 0.5 h at 150 °C. All the films were then removed from the NaCl substrate by dissolving it in water, and placed on annealed copper grids, the grid bars of which were precoated with the solution used to cast the original film. After drying (in air a few hours and again in a vacuum for about 6 h) the films containing aromatic amines were cured 2.5 h at 150 °C while those containing aliphatic amines were cured at 100 °C for a time sufficient to bring their total cure time to 3 h. During this final cure the film was bonded to the grid and any wrinkles present disappeared. Nearly the same procedure was followed for the M_R = 40k and M_R = 70k DGEBA resins except that they were not cured. Films of these resins were bonded to the grids by a short exposure to solvent vapour [23] after which the grids were given a final vacuum treatment to remove solvent.

In the course of these investigations it became desirable to prepare epoxy networks with even smaller strand densities than that of the entanglement network of high molecular weight DGEBA. For this purpose a set of diluted epoxies was prepared using MDA as the curing agent. An appropriate diluent will neither crosslink nor entangle with the network strands. One possible molecule with these properties (and one with little interaction with the DGEBA network) is a small non-reactive DGEBA molecule. Such a diluent was made by reacting $M_R = 1850$ DGEBA with phenol at 135 °C for 8 h using benzyldimethylamine as a catalyst. The resulting molecule has its ends capped with phenyl groups instead of epoxide groups [24] and will not participate in the curing reaction with MDA. The absence of epoxide groups on the diluent was verified by observing the infrared absorption peak at 918 cm^{-1}, which is due to an asymmetric stretch of the oxirane ring [25, 26]. After mixing different proportions of reactive and non-reactive resins with MDA, the spun solution was cured to produce thin films using the procedure outlined above for the undiluted epoxies. Instead of a precure on the NaCl substrate, the film was given a final cure on the NaCl for 24 h at 150 °C. Subsequent bonding to the grid was achieved by heating the sample to a temperature just above T_g for a short time (0.5 to 1 h).

To examine the effects of stoichiometry additional samples were crosslinked with amounts of MDA which corresponded to various fractions, f, of the stoichiometric value. Besides providing another way to decrease the strand density of the original epoxies, these samples should provide points of comparison with the many previous studies of the effects of varying the stoichiometry on the macroscopic mechanical properties of epoxies.

In order to create a reproducible nucleation site for plastic deformation, microcracks approximately 10 μm wide and 80 μm long were burned in the centre of each of the film squares in all of the samples using the intense electron beam of an electron microprobe. The grids were strained by hand in tension until plastic zones of suitable size were observed in the epoxy films by optical microscopy, after which the copper grid square containing the desired plastic zone was cut out. The plastic deformation of the copper grid bars holds the polymer film under tension while it is observed with transmission electron microscopy (TEM).

The optical densities of various regions on the TEM micrographs were measured with an optical microdensitometer. The optical density measurements were converted to a thickness (or volume) fraction, v_f, of the deformed material in the DZ (or craze) using

$$v_f = 1 - \frac{\ln(\Phi_{DZ}/\Phi_{film})}{\ln(\Phi_{hole}/\Phi_{film})} \quad (12)$$

where Φ_{hole}, Φ_{film}, and Φ_{DZ} are the optical densities of the probe hole, the surrounding polymer film, and the DZ (or craze), respectively [23, 27]. Since volume is conserved during plastic deformation the extension ratio of the DZ or craze is given by

$$\lambda = 1/v_f \quad (13)$$

While the network parameters may be computed based on simple assumptions it is necessary to verify these calculations with direct measurements in crosslinked networks such as epoxies. Consequently, the network strand density was determined by measuring G_N^0, the shear modulus on the rubbery plateau. The strand density was computed from the theory of rubber elasticity [28] to be

$$\nu = G_N^0/k_B T \quad (14)$$

where k_B is Boltzman's constant and T is the absolute temperature. Measurements of G_N^0 are expected to produce values of ν with contributions from both trapped entanglements and cross-links [29].

For such measurements of G_N^0 samples ranging in thickness from 0.25 to 0.35 mm were prepared by casting. Viscous solutions of MDA and DGEBA in methyl ethyl ketone (MEK) were made and applied to a polished Teflon substrate on which thick spacers were placed along opposite edges. Scraping a razor blade across the top of the spacers produced a sample with relatively uniform thickness. The samples were partially dried by placing in undersaturated MEK vapour for 4 days to minimize bubble formation which resulted from the MEK evaporating too quickly, and then allowed to dry in air for an additional two days. In spite of these precautions a few bubbles remained in the sheets although their presence did not significantly affect the results. In order to remove excess solvent (still limiting the evaporation rate) the sheets were heated to 55 °C for 3 h and finally cured at 150 °C for 2.5 h if undiluted and for 24 h if diluted. The 3.6k DGEBA contained more solvent than any other sample, thus it was given an additional thermal treatment just prior to curing of 4 h at 80 °C. Similarly, the diluted samples were heated for a total of 16 h at 55 °C and 9 h at 80 °C before they were cured. Specimens 1 to 2 cm long and 0.4 cm wide were cut from the cast sheet. Based on a polymer density of 1.16 $g\,cm^{-3}$ the cross-sectional area of each sample was calculated by measuring its length and its mass. The shear modulus of these samples was measured as a function of temperature using a Rheovibron (model DDV-II, Tokyo Instruments) at 110 Hz with an oscillating displacement of 0.016 mm applied in tension along the samples. The result of one measurement is shown in Fig. 1. All the samples exhibited both a sharp drop in shear modulus, G, of approximately two orders in magnitude when passing through their glass transition, T_g, and a relatively constant G above T_g. The modulus, G_{N^0}, at 180 °C on this rubbery plateau was used for the calculations of ν.

In order to estimate qualitatively the fracture toughness of the epoxy films, copper grids were strained with a motorized strain frame at a nominal strain rate of 1.5% h^{-1}. A typical grid contained approximately 20 to 25 grid squares which had epoxy film extending across them. Samples both with preexisting probe holes and without them were tested. In each grid square the fraction of squares in which a DZ

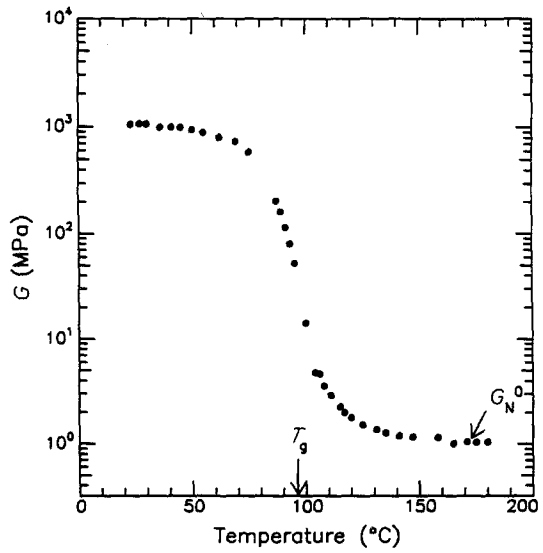

Figure 1 A typical plot of shear modulus, G, against temperature, T, for a cross-linked epoxy. Marked are the glass transition temperature, T_g, and the value for the rubbery shear modulus, G_N^0, used in calculations of the strand density.

and a crack had formed, and in which a crack had grown 0.12, 0.23, and 0.35 mm was recorded as a function of true strain.

4. Results

4.1. Network parameters

The rubbery shear modulus, G_N^0, of various epoxies is displayed in Table I. Note that as expected, G_N^0 decreases with increasing molecular weight of the starting DGEBA resin for undiluted network ($\chi = 1.0$). The network strand densities, ν, and strand molecular weights, M, are computed from Equation 14 and

$$M = \rho N_A/\nu \tag{15}$$

respectively. (Equation 15 is a generalized version of Equation 1 for which it is assumed that network strands terminate either in entanglements or cross-links.) As expected, for the undiluted networks, the strand molecular weight is always larger than the DGEBA resin molecular weight since some of the chemically formed strands are elastically inactive.

Some measurements of the diluted networks are also included in Table I. In this case the strand molecular weights are extracted from the G_N^0s using

$$M = \chi\rho N_A k_B T/G_N^0 \tag{16}$$

where the $\chi\rho$ in the numerator is an effective polymer strand density. It is necessary to include only the network strands (and not the diluent molecules) in the theory of rubber elasticity. Note that for the diluted networks the νs are less than, and the Ms greater than, those for the corresponding undiluted epoxy. Also shown in Table I are the strand densities, ν^*, and the strand molecular weights, M^*, of the various diluted epoxies estimated using*

$$\nu^*(\chi) = \chi^2\nu(\chi = 1) \tag{17a}$$

$$M^*(\chi) = M\ (\chi = 1)/\chi \tag{17b}$$

These estimates became necessary because of the difficulties of accurately measuring G_N^0 in the highly diluted epoxies. The agreement between the measured and extrapolated values of M is only fair, but within the uncertainty of the measurements of the small G_N^0s.

4.2. Microdeformation

The deformed epoxy films were examined by optical and transmission electron microscopy. Crazes were never observed in any of the undiluted epoxies. These films deformed only by nucleation and growth of plane stress deformation zones. Figs 2a and b show optical micrographs of the DZs in the lowest M_R (= 350) epoxy and in an intermediate M_R (= 1050) epoxy. Both films were cross-linked with MDA. The DZ in the higher M_R epoxy has sharp edges whereas the DZ in the lower M_R epoxy has no obvious boundaries. Fig. 2c shows a DZ in a diluted epoxy (M_R = 3600, $\chi = 0.50$). Even at this dilution no crazes are observed. Optically, this DZ appears similar to that in

TABLE I The shear moduli, G_N^0, the strand densities, ν and ν^*, and the strand molecular weights, M and M^*, for a series of epoxies made from resins with initial molecular weight, M_R, and weight fraction, χ

Resin weight, M_R	χ	G_N^0 (MPa)	ν (10^{25} m^{-3})	M	$\nu^* = \chi^2\nu(\chi = 1)$ (10^{25} m^{-3})	$M^* = M(\chi = 1)/\chi$
350	1.0	8.45	135	520		
500	1.0	6.3	100	690		
1050	1.0	2.4	38	1800		
1850	1.0	2.1	33.5	2100		
3600	1.0	0.82	13	5350		
1050	0.5	1.0	16	2200	9.5	3650
1050	0.7				19	2600
1850	0.5	0.5	8.0	4400	8.4	4150
1850	0.70				16.4	3000
1850	0.85				24.2	2450
3600	0.5				3.3	10700
3600	0.6				4.7	8900
3600	0.7	0.3	4.8	10200	6.4	7650
3600	0.85				9.4	6300

* These expressions assume that the diluent chains do not swell the polymer. The change in λ, however, has been shown to be negligible in this region of ν even if the diluent acts as a good solvent [13].

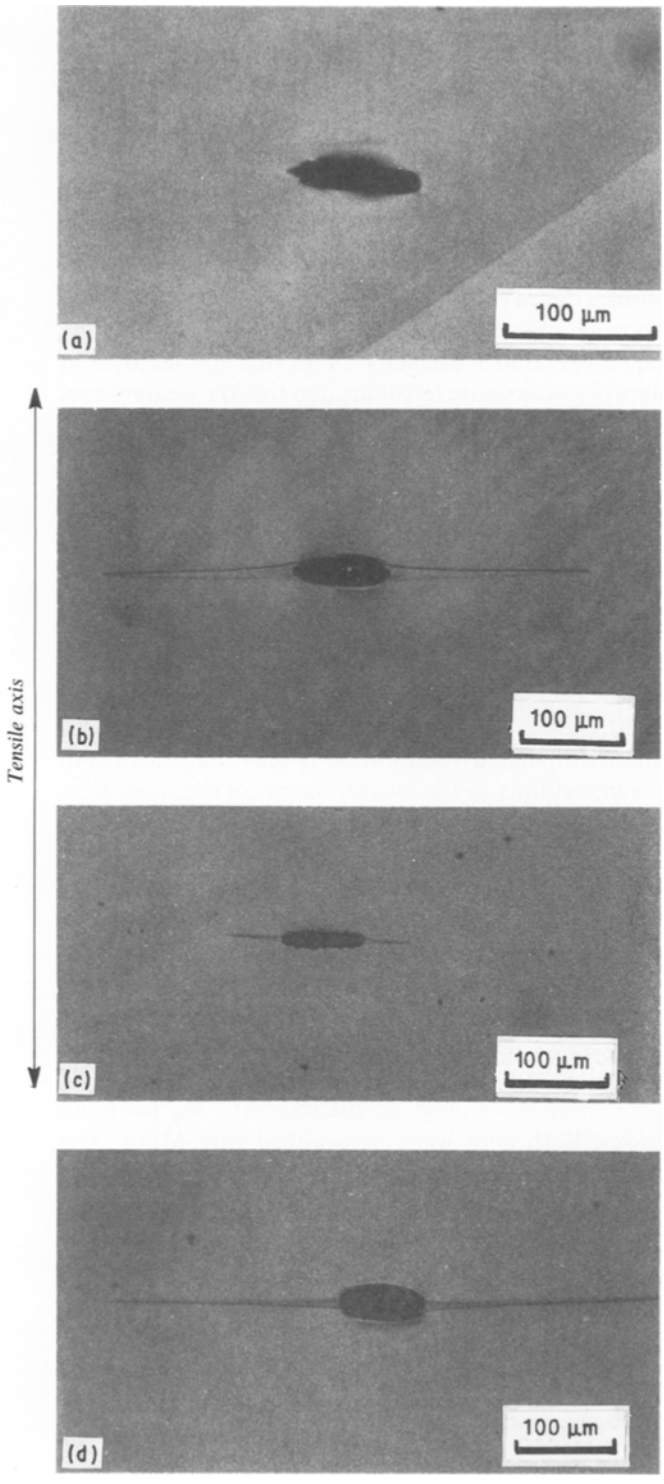

Figure 2 Optical micrographs of deformation zones in a series of DGEBA epoxies. (a) $M_R = 350$, cross-linked epoxy. (b) $M_R = 1050$, crosslinked epoxy. (c) $M_R = 3600$, diluted cross-linked epoxy with $\chi = 0.50$. (d) $M_R = 70$k, uncross-linked phenoxy. Also observed are the cracks used for DZ initiation sites.

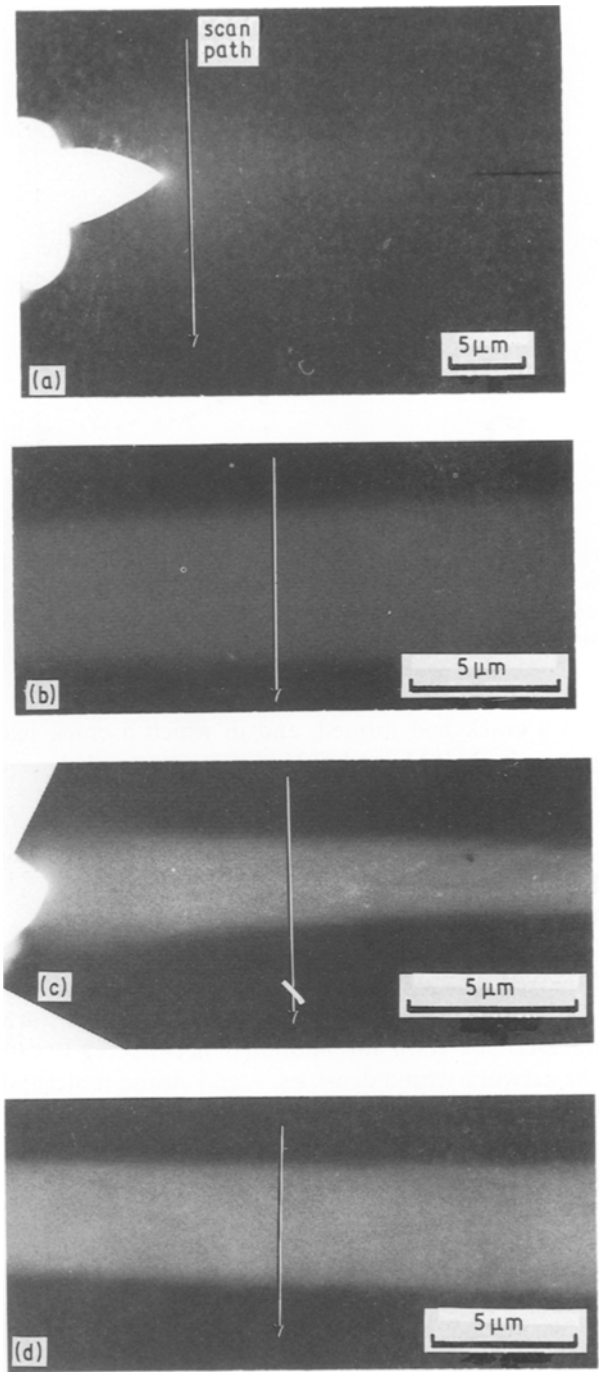

Figure 3 The TEM micrographs corresponding to the DZs displayed in Fig. 2. (a) $M_R = 350$, cross-linked epoxy. (b) $M_R = 1050$, cross-linked epoxy. (c) $M_R = 3600$, diluted cross-linked epoxy with $\chi = 0.50$. (d) $M_R = 70$k, uncross-linked phenoxy. Shown also are the paths of the microdensitometer scan used to generate optical density traces.

Fig. 2b, the undiluted intermediate M_R epoxy. Fig. 2d shows that even in the $M_R = 70$k phenoxy resin where the strands are only entangled and not cross-linked, only DZs form.

Transmission electron microscopy can further illuminate these changes in the character of the DZs with decreasing strand density. TEM micrographs of the DZs in Fig. 2 are shown in Fig. 3. The diffuse character of the zone edges in the $M_R = 350$ epoxy is apparent as is a pronounced increase in the contrast between the DZ and the (undeformed) surrounding film as M increases and ν decreases. The DZ extension ratio versus the distance across the DZ along paths marked on Fig. 3 is displayed in Fig. 4. These values of λ were computed from microdensitometer scans of the image plates using Equations 12 and 13.

The λ against distance curves confirm the qualitative observations of the diffuse character of the DZ in the most highly cross-linked epoxy and the sharp nature of the edges of the DZ in the less highly cross-linked ones. The most important trend, however, is the increase in the characteristic extension ratio, λ, (in the centre of the DZ) from approximately 1.2 for the

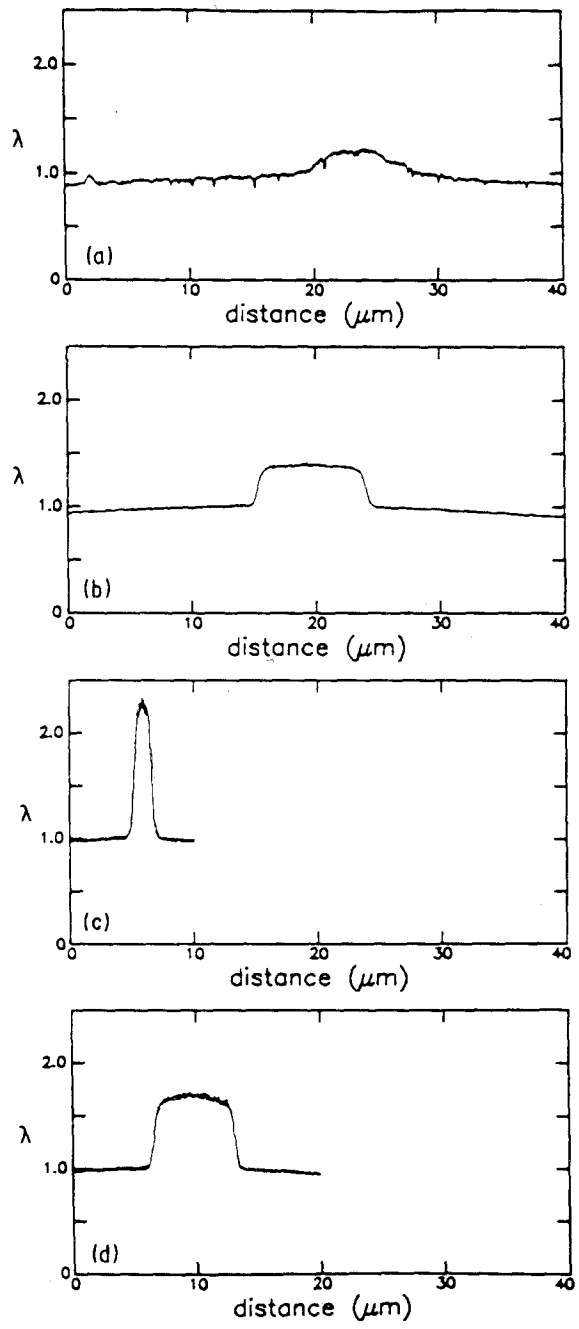

Figure 4 Extension ratio, λ, against distance curves for the epoxies displayed in Figs 2 and 3. The curves were computed from the optical density traces taken along the paths marked in Fig. 3 using Equations 12 and 13. (a) $M_R = 350$, cross-linked epoxy. (b) $M_R = 1050$, cross-linked epoxy. (c) $M_R = 3600$, diluted cross-linked epoxy with $\chi = 0.50$. (d) $M_R = 70$k, uncross-linked phenoxy.

$M_R = 350$ epoxy to approximately 1.4 for the $M_R = 1050$ epoxy to approximately 2.3 for the diluted $M_R = 3600$ epoxy. The uncross-linked $M_R = 70$k epoxy has a λ of 1.7 which is less than that of the diluted epoxy but greater than those for the undiluted cross-linked epoxies. Clearly, for epoxies, as for thermoplastics and cross-linked polystyrene, λ increases with decreasing network strand density.

This qualitative conclusion is further supported by the data for all the samples displayed in Fig. 5. The circles represent the data for undiluted epoxies cross-linked with MDA while the triangles and the diamonds represent the ν* and ν from the diluted epoxies in Table I (also crosslinked with MDA). The extension ratio λ clearly increases monotonically with decreasing network strand density.

For some of the DGEBA epoxies the MDA cross-linking agent was decreased to a fraction, f, of its stoichiometric value. Again, even though ν must be reduced by decreasing f, only DZs were observed in such films. No crazes were detected. The extension ratios in non-stoichiometric epoxies with two different resin molecular weights, circles corresponding to $M_R = 1850$ and triangles corresponding to $M_R = 350$, are shown in Fig. 6. While the DZ extension ratio is less sensitive to non-stoichiometry than to either resin molecular weight or diluent concentration, λ does increase as ν is decreased by decreasing f.

The sizes of the cross-linking amine molecules are much smaller than the starting DGEBA chains. One

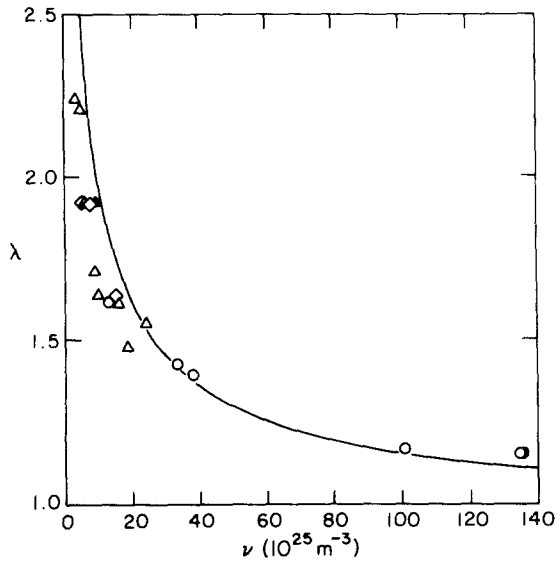

Figure 5 Extension ratio, λ, plotted against strand density, ν. (○, undiluted epoxies using ν computed from Equation 14; ◇, diluted epoxies using ν computed from Equations 15 and 16; △, diluted epoxies using ν* computed from Equation 17a.

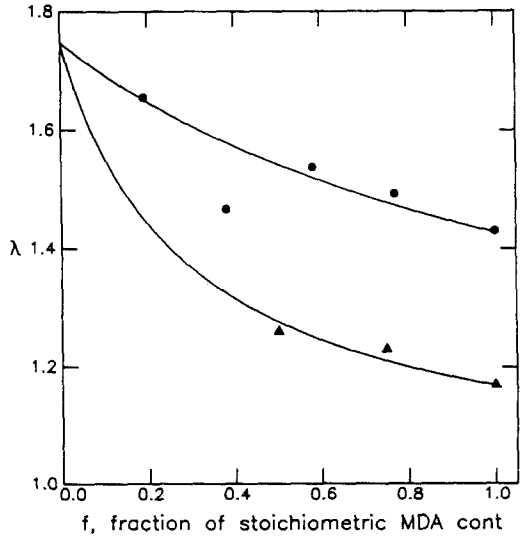

Figure 6 Extension ratio, λ, plotted against fraction of stoichiometric MDA content, f, for two sets of initial resin molecular weights. (○, $M_R = 1850$; △, $M_R = 350$. The curves are computed from strand densities given by Equation. 20.

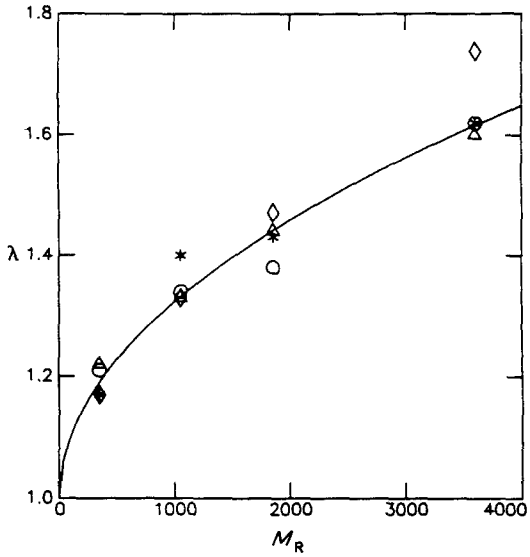

Figure 7 Extension ratio, λ, for epoxies produced using a series of amine curing agents, plotted against resin molecular weight, M_R. (*, MDA; ◇, MPDA; △, DETA; ○, TEPA.)

might expect, therefore, that different amine cross-linking agents would produce similar results for a given starting DGEBA resin molecular weight. Fig. 7, where λ is plotted against M_R for various amine cross-linking agents, shows that this expectation is borne out. The asterisks, diamonds, triangles, and circles represent epoxies cross-linked with MDA, MPDA, DETA, and TEPA, respectively. There is no systematic variation in λ with cross-linking agent.

While no crazes were observed in any of the cross-linked epoxies or in the undiluted phenoxy resins, crazes were seen in one diluted phenoxy resin (M_R=40k, $\chi = 0.75$). No crazes were seen in diluted films of the other M_R = 70k phenoxy resin.

Besides strongly affecting the extension ratios in DZs in these epoxies, the network strand density also influences the initiation strains of the DZs. Fig. 8 contains the results of a constant extension rate measurement on an M_R = 1050, MDA cross-linked epoxy. In Fig. 8a the fraction, P, of grid squares in which DZs

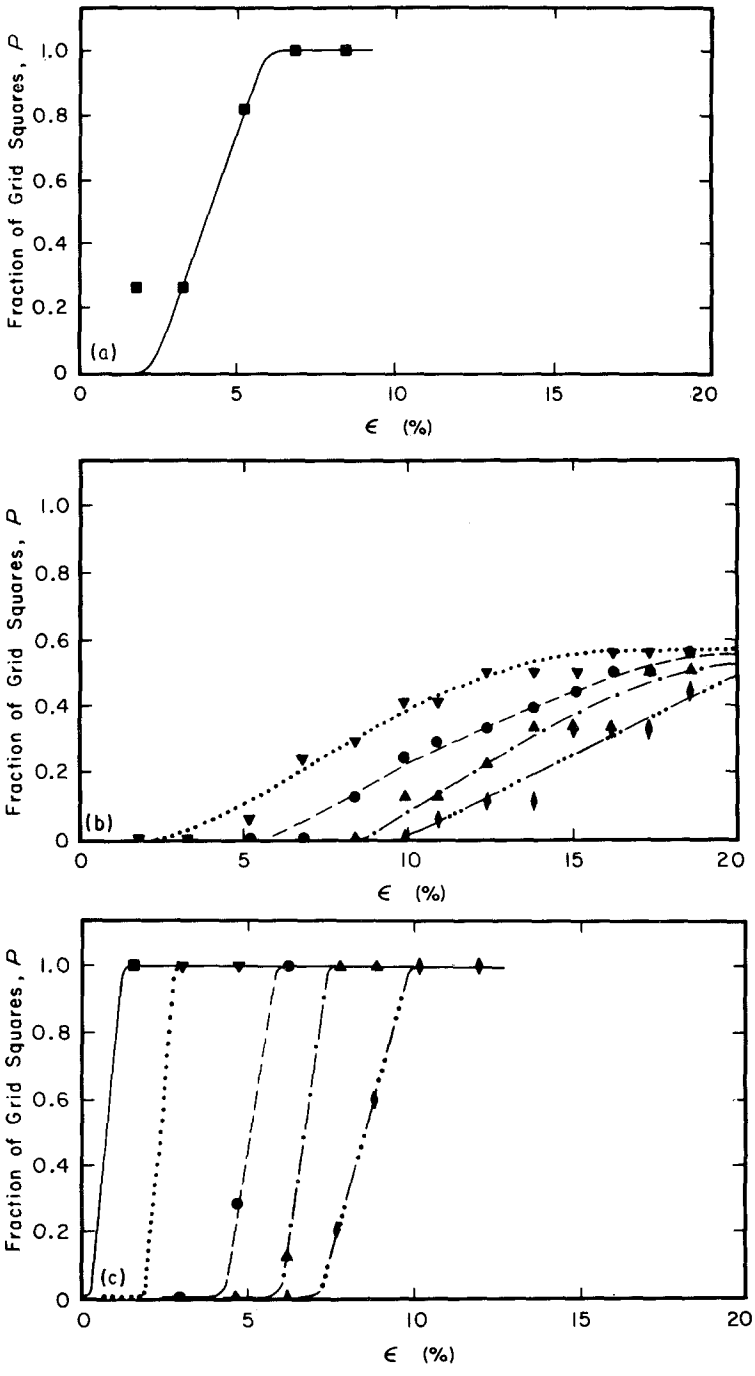

Figure 8 The fraction of grid squares, P, in which a given deformation event is observed in an M_R = 1050 epoxy film, plotted against true strain, ε. The films were deformed both with starter cracks and without. (a) fraction of squares, P, in which DZs have been initiated in a film with no starter cracks, plotted against ε. (b) fraction of squares, P, in which cracks have grown to various lengths in a film with no starter cracks, plotted against ε. (....., ▼, crack initiation; – –, ●, 0.12 mm; –·–·, ▲, 0.23 mm; –···–···, ◆, 0.35 mm.) (c) fraction of squares, P, in which DZs and cracks have initiated, and in which cracks have grown to various lengths, in a film with starter cracks, plotted against ε. (—, ■, DZ initiation; ....., ▼, crack initiation; – –, ●, 0.12 mm; –·–·, ▲, 0.23 mm; –···–···, ◆, 0.35 mm.)

are observed in a film containing no pre-existing probe holes is plotted against the true strain of the film. The strain at which $P = 0.25$ may be used as a critical strain in order to compare the nucleation of observable regions of localized strain of the different epoxies. Fig. 9 contains the results of this comparison, where the critical strain, ε_c, is plotted against M_R. Obviously, low ν (high M_R) epoxies are more prone to strain localization than high ν epoxies. This trend is to be expected in light of the increased strain hardening of the high ν epoxies.

4.3. Fracture

Since the fracture toughness in these thin films results primarily from the plastic deformation at the crack tips, a qualitative estimate of it may be obtained from monitoring the crack growth into the DZ. One might expect the higher λ_{max} epoxies to contain cracks which, at a given strain, are shorter due to the higher amounts of plastic deformation necessary to form the DZs ahead of them. In Figs 2a and b, for roughly equal amounts of strain, the proportion of crack length to DZ length is markedly different, with the high ν epoxy deforming very little before crack growth is initiated. This trend is borne out by more quantitative studies of crack propagation in the undiluted epoxies. Fig. 8b contains the results of a measurement on an $M_R = 1050$, MDA cross-linked epoxy with no pre-existing starter crack, where the fraction of grid squares, P, in which the crack length has reached a given value is plotted against true strain. The inverted triangles represent the initiation of crack growth, while the circles, triangles and diamonds represent crack lengths of 0.12, 0.23, and 0.35 mm, respectively. Although some of the DZs have not yet begun to break down, even at strains as high as 20%, cracks grown from those that have are already near the edge of the grid squares at these high strains.

The results for an $M_R = 1050$ epoxy film with starter cracks introduced prior to straining are presented in Fig. 8c, where the symbols representing each stage

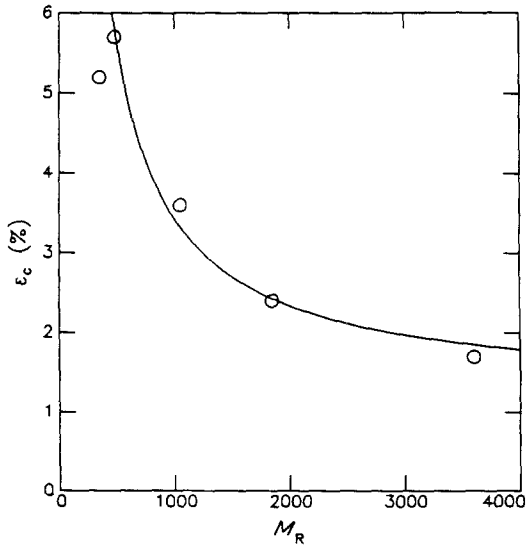

Figure 9 The critical strain for DZ formation, ε_c, plotted against the initial resin molecular weight, M_R.

of the deformation correspond to those in Figs 8a and b. When nucleation holes exist, there is only a small incubation strain (time) associated with the initiation of crack propagation. This behaviour is to be contrasted with the behaviour of the films with no starter crack, which have a significantly larger incubation strain. In Fig. 10, crack length is plotted against true strain for films both with starter cracks (squares) and without (circles), for each of the M_Rs. Crack initiation is observed in only some of the grid squares without starter cracks, and the crack initiation in a given grid square appears to depend more on the perfection of the film than on M_R, thus the strain measured and plotted in Fig. 10 is the strain at which 0.25 of the squares in which cracks have initiated exhibit the given crack lengths. As expected, the crack lengths for a given strain decrease with decreasing strand density, and hence, the fracture toughness increases with this change in ν. Note that once crack initiation has taken place the crack growth in both sets of films is similar.

Similar qualitative observations may be made of the diluted epoxies while straining them by hand. The tendency for increased strain localization in low ν epoxies is continued in the diluted samples, where DZ formation is observed at strains of approximately 0.5% or less in samples (e.g., $M_R = 3600$, $\chi = 0.50$) without probe holes. Furthermore, these DZs in the diluted epoxies break down sooner to form cracks than those in the undiluted epoxies. In experiments with holes and without, two levels of this breakdown exist, related to the amount of dilution. At low and moderate dilutions (e.g., $M_R = 1050$, $0.50 < \chi < 1.0$, or $M_R = 3600$, $0.70 < \chi < 1.0$), DZ growth to a maximum length of 0.50 mm limited by the grid size easily occurs, and the crack propagation is reasonably stable. The crack growth may be initiated either from the starter crack, or from within the DZ. At high dilutions (e.g., $M_R = 3600$, $0.5 < \chi < 0.7$), the crack propagation is highly unstable. After the DZ has grown only to a length of ≈ 0.10 mm, any further straining will likely result in catastrophic fracture of the film by rapid crack propagation followed by crack branching. An example of a DZ beginning to break down into a crack, a precursor to this fracture, is presented in Fig. 11 for a highly diluted ($M_R = 3600$, $\chi = 0.50$) epoxy. In addition, the initiation site for this pattern is frequently well away from the main starter crack and the initial DZ nucleation site. The dramatic effect of dilution on the fracture properties of epoxies, similarly observed in some thermoplastics [12, 13] is further illustrated in Fig. 12 where the crack length is plotted against strain for three constant extension rate experiments on an $M_R = 3600$ epoxy. The squares and circles represent values of dilution corresponding to $\chi = 0.50$ and 0.85, respectively, while the triangles represent the undiluted epoxy ($\chi = 1.0$). The crack length is seen to increase with increasing dilution (decreasing χ).

5. Discussion

If the network model is correct one expects the extension ratio of the DZs to be correlated with λ_{max}, the

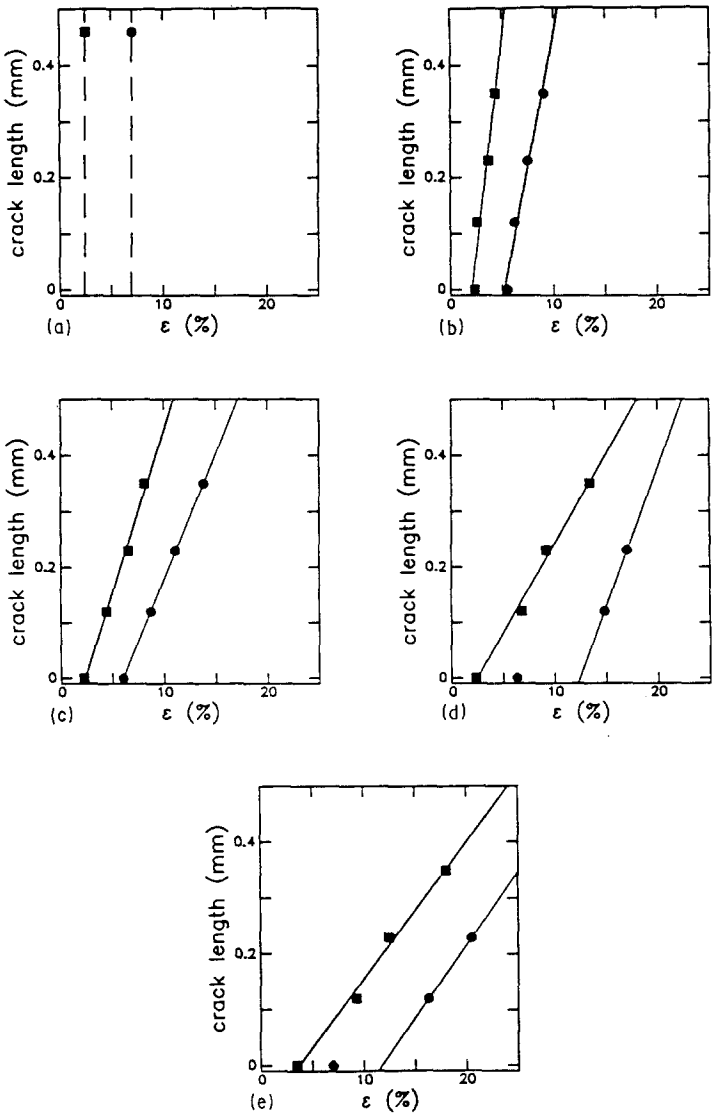

Figure 10 Plots of crack length against true strain for films both with starter cracks (■) and without (●). (a) $M_R = 350$ epoxy. (b) $M_R = 500$ epoxy. (c) $M_R = 1050$ epoxy. (d) $M_R = 1850$ epoxy. (e) $M_R = 3600$ epoxy.

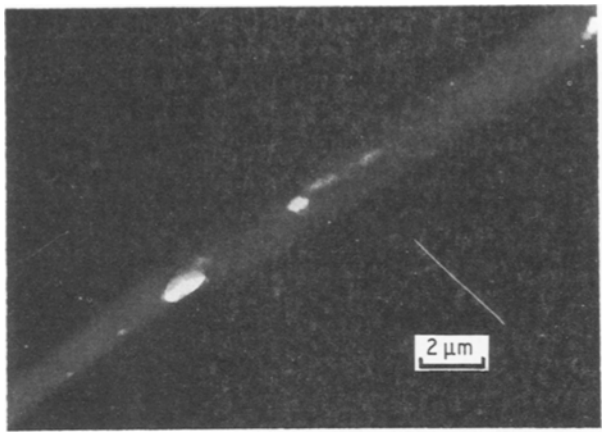

Figure 11 TEM micrograph of a DZ in a diluted $M_R = 3600$ epoxy ($\chi = 0.50$), where the DZ has begun to break down to form a crack. The strain is less than 1%.

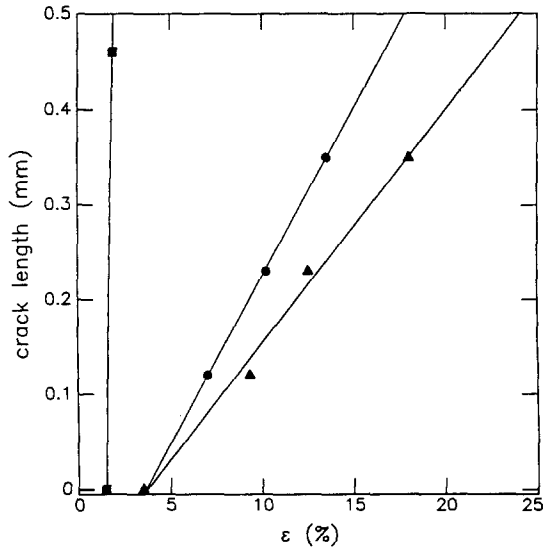

Figure 12 Plot of crack length against true strain for a series of $M_R = 3600$ epoxies. (■, diluted, $\chi = 0.50$; ●, diluted, $\chi = 0.85$; ▲ undiluted, $\chi = 1.0$). The crack size for $\chi = 0.50$ was limited by the size of the grid square. There was no stable growth at this dilution level.

maximum extension ratio of an individual strand in the network. While it is not expected that individual strands are stretched taut, the onset of strong strain hardening due to polymer chain orientation should scale with λ_{max}. Fig. 13 shows a plot of $\lambda - 1$ against $\lambda_{max} - 1$. The λ_{max} has been calculated using the Kratky–Porod model of a worm-like chain (Equations 2–6) and the two sets of Ms from Table I. The symbols have the same meaning as those in Fig. 5. The data may be represented by the relation

$$(\lambda - 1) = 0.32(\lambda_{max} - 1) \quad (18)$$

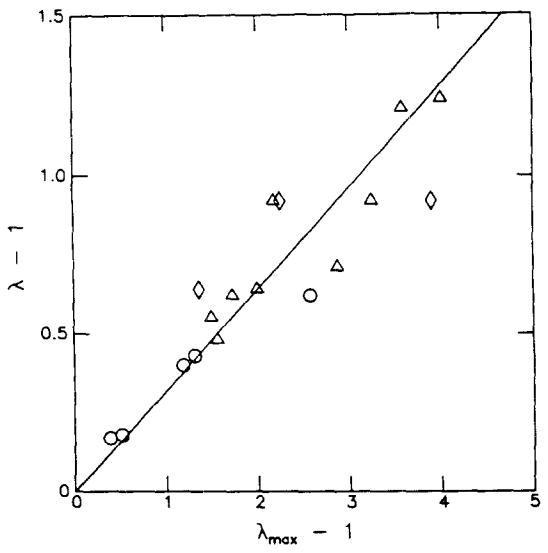

Figure 13 A plot of $\lambda - 1$ against $\lambda_{max} - 1$, where λ_{max} was computed from M using Equations 2 to 6. (○, undiluted epoxies using M computed from Equations 14 and 15; ◇, diluted epoxies using M computed from Equation 16; △, diluted epoxies using M* computed from Equation 17b.)

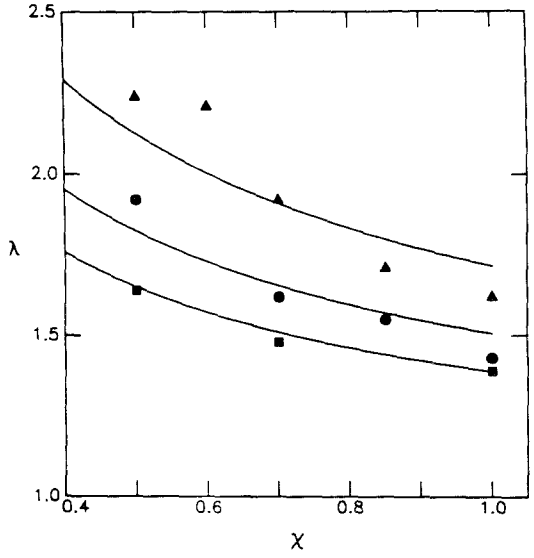

Figure 14 A plot of λ against χ for three different M_R epoxies. (■, M_R = 1050 epoxy; ●, M_R = 1850 epoxy; ▲, M_R = 3600 epoxy.

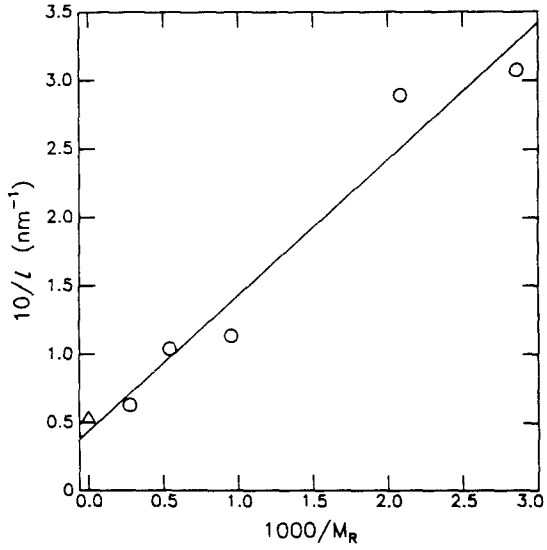

Figure 15 A plot $10/l$ against $1000/M_R$, where l and M_R are the average strand contour length and initial resin molecular weight, respectively. The slope and intercept correspond to $\alpha = 0.45$ and $l_E = 23$ nm.

which, also drawn in Fig. 13, is close to that found for cross-linked polystyrene, [15] i.e., $(\lambda - 1) = 0.40(\lambda_{max} - 1)$. Clearly there is an excellent correlation between the extension ratio in the deformation zone and the maximum extension ratio of a single strand in the epoxy network. This correlation is used to create a curve relating λ and ν. The strand length, l, is computed from Equations 1 and 2 and converted to λ_{max} using Equations 3 to 6, and then to λ using Equation 18. The resulting theoretical fit is drawn on Fig. 5, with good agreement.

The diluted epoxy networks show the same correlation as the undiluted ones. This fact is brought out more directly by Fig. 14 in which λ is plotted against χ, the weight fraction of network chains for several molecular weights of starting DGEBA. The solid lines are computed from Equation 18 with λ_{max} computed from Equations 2 to 6 and 17b. A best fit was used to determine the value for $M(\chi = 1)$ to be used in Equation 17b. The agreement is reasonable.

An important question that is not answered directly by Figs 13 and 14 is what is the contribution of entanglements between DGEBA chains to the network. The value of M measured from G_{N^0} contains contributions from both crosslinked and entangled strands. The entanglement portion of M may be obtained from the entanglement molecular weight of the linear phenoxy strands which in turn may be inferred from the λ of DZs in the linear phenoxy. The λ of DZs in both the M_R = 40k and M_R = 70k DGEBA (phenoxy) was 1.7. From this value, a λ_{max} of 3.2 can be computed from Equation 18 for the entangled DGEBA strands which corresponds to an l_E of approximately 19 nm and an entanglement molecular weight of 4200.

A second method to find the effects of entanglements is to extrapolate the results of the cross-linked networks which contain trapped entangled strands, giving a total strand density $\nu = \nu_E + \nu_X$ (Equation 7). Equation 8 may be rewritten as

$$1/l = 1/l_E + \alpha(M_0/l_0)(1/M_R), \qquad (19)$$

where α represents the fraction of chemically reacted strands that are effective network strands. The value of α should be less than 1 since not all the reacted DGEBA molecules will become elastically active strands in the network [30–33]. Values of $1/l$ extracted from the λ measurements via Equations 18 and 2 to 6 are plotted against $1/M_R$ in Fig. 15*. The slope results in a value of $\alpha = 0.45$ and the intercept gives values of l_E and M_E equal to 23 nm and 5050 daltons, respectively. These values are close to those inferred directly from the purely entangled DGEBA,

* Since λ is independent of these amine curing agents, we assume that the deformation is occurring predominantly by the orientation of the DGEBA molecules, hence the size of the MDA molecule is ignored in the calculation of M_R.

but twice the values computed from measurements of G_{N^0}, which yield an M_E of approximately 2200 [34].

Thus established, the entanglement network may be used to infer the changes that occur in the network structures of the non-stoichiometric epoxies. In Fig. 6, the extension ratio of these epoxies never rises above that of an uncrosslinked phenoxy, suggesting that entanglements play an important role in MDA deficient epoxies. To predict these extension ratios, the measured values of λ for $f = 1.0$ for the two epoxies studied ($M_R = 350$ and $M_R = 1850$) were converted to values of λ_{max} using Equation 18. Values of l were extracted from these λ_{max} using Equations 2 to 6. The entanglement and crosslinked contributions to this contour length were separated using Equations 8 and 7 whereby the strand density in a non-stoichiometric epoxy was computed using*

$$\nu(f) = \nu_E + f\nu_X (f = 1). \quad (20)$$

The extension ratio in this epoxy, $\lambda(f)$, was calculated by converting the $\nu(f)$ from Equation 20 to an $l(f)$ using Equations 15 and 2. After $\lambda_{max}(f)$ was computed from $l(f)$ using Equation 3, it was converted to $\lambda(f)$ from the empirical relation in Equation 18. Fig. 6 shows the theoretical curves derived from this treatment. The agreement is excellent.

The extension ratio of the DZs is found to be independent of the choice of curing agent. In retrospect such independence should be expected. From the simple theory, only if substituting different curing agents affects l, the contour distance between network points, will it affect λ. Even in the lowest M_R (= 350) epoxy, the differences in l produced by capping the ends of the DGEBA resin with the different amines are very small. For the higher M_R epoxies these differences are even less.

Materials with higher strain hardening capabilities will resist strain localization until higher strains. Since the strain hardening in these epoxies is due directly to the orientation of the network strands, the DZ initiation strain should (and does) increase with increasing strand density. The fracture behavior, however, is related both to the initiation of a plastic zone and a crack, and, once initiated, to the propagation of the zone and the crack behind it. It is seen qualitatively that as ν is increased in the undiluted epoxies, the crack lengths behind the DZs are shorter for a given amount of strain, and that, therefore, the fracture toughness is increased. In order to confirm this trend,

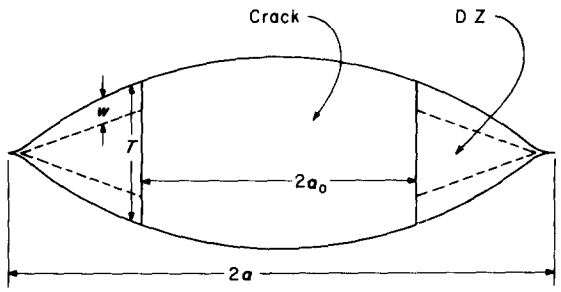

Figure 16 Schematic of a crack and the DZ growing ahead of it.

the Dugdale model [36, 37] may be used to estimate quantitatively values for the plain stress fracture toughness, G_C. In Fig. 16, a schematic of a crack and the DZ ahead of it are shown, where T is its current width. The displacement of each border of the DZ is given by [23]

$$w = (T/2)(1 - 1/\lambda) \quad (21)$$

If the DZ grows with a steady state displacement profile, $w(x)$, ahead of the propagating crack, the critical energy release rate G_C, may be written as

$$G_C = -2\int_{a_0}^{a} \sigma(x)\frac{dw}{dx}dx = 2\int_0^{w_C} \sigma dw \quad (22)$$

where $\sigma(x)$ is the stress profile along the DZ, a_0 and a are the half-lengths of the crack and of the crack + DZ, respectively, and w_C is the crack opening displacement. The Dugdale model assumes that the stress along the DZ is a constant value, σ_y, giving

$$G_C = 2\sigma_y w_C. \quad (23)$$

Substituting measured values for the yield stress [38] and for w_C (measured during the constant extension rate experiments) gives the G_Cs displayed in Table II. The decrease in yield stress with decreasing strand density is more than counteracted by the accompanying increase in w_C, resulting in an overall increase in G_C with decreasing ν. These results are in qualitative agreement with recent measurements [35, 39, 40] for similar epoxies which show that the plane strain fracture toughness (corresponding to crack arrest) increases as $M_c^{0.5}$.

Since diluting the network decreases the number of load bearing chains, decreasing ν in this fashion decreases rather than increases the fracture toughness. In a DZ, where the chains are highly oriented and lined

*This assumption is justified in epoxy systems that have f significantly greater than f_c, where f_c is a critical fraction for the epoxy to form a gel upon cross-linking. For a condensation polymerization, such as the cross-linking reaction between DGEBA and MDA, the gel point is given by [30]

$$f_c p^2 = 1/(f^* - 1)$$

where p is the probability that an MDA amine group will react and f^* is the functionality of the MDA molecule. We assume that all MDA groups are exhausted. Therefore $f_c = 1/3$ and the extension ratio in the non-stoichiometric $M_R = 350$ epoxies, where $f \geqslant 0.50$, should be described by Equation 20. The $M_R = 1850$ epoxies, however, have fs of 0.40 and 0.20 which are close to or less than the gel point. Even the smallest star structures formed during cure in these systems, containing only one MDA molecule and four DGEBA molecules, are large enough to entangle with the network. If all the MDA molecules were not "linked" together, a situation similar to the dilution experiments would exist and these small star polymers would be diluting the entanglement network; clearly this dilution effect is not observed. For the $M_R = 1850$ epoxy with $f < 0.25$, presumably there would be a slight dilution effect with $\chi = 1.0-(0.25 - f)$. We ignore this for $f = 0.18$. For the $M_R = 350$ epoxy, one might expect some sol fraction at $f = 0.50$. The sol fraction has been measured [35] for $f = 0.65$ to be 12%. Theoretically, some of these sol molecules would be long enough to entangle and therefore contribute to ν, however, large amounts of unreacted $M_R = 350$ DGEBA resin were found in the sol. In any case, we also neglect this small effect.

TABLE II The plane stress fracture toughness, G_C, for different M_R epoxies

Resin molecular weight, M_R	G_C (J m^{-2})
500	360 ± 45
1050	300 ± 20
1850	430 ± 65
3600	530 ± 50

up along the DZ edge, the area per chain is constant with ν for the undiluted networks. Diluting the network, however, dramatically increases the force per chain in the DZ due to an increase in area per load bearing chain. Since the true stress within the DZ is given by $\lambda\sigma_y$, and since λ varies approximately as $\chi^{-1/2}$, the force per load bearing strand increases as $\chi^{-3/2}$. This increase in load means that instead of promoting a shear to craze transition, diluting the network induces fracture to occur.

A major conclusion of this paper is that epoxies do not craze readily. Crazes were observed only in films of the diluted uncross-linked M_R = 40k phenoxy resin. These crazes, however, are attributed to the ability of the M_R = 40k phenoxy to disentangle because of its shorter chain length. No crazes were observed in the diluted longer chain M_R = 70k phenoxies. Fig. 17 is a revised version of Henkee and Kramer's Fig. 8 [15] which shows the competition between shear deformation and crazing for glassy polymers but now includes our results on epoxies. Our observations are consistent with the predictions of the network model which dictate that the increase in fibril surface energy, Γ, with strand density predicted by Equation 9 will inhibit crazing relative to shear deformation in polymers with as high strand densities as epoxies. While one might naively expect to be able to produce crazing even in epoxies by diluting the network sufficiently, such diluted networks become so fragile due to the extreme dilution of load bearing chains that only cracks and not crazes are observed.

These observations are in direct conflict with those of Morgan [2] who reports the presence of crazes in both macroscopic and thin film epoxies. The resin molecular weight used by Morgan corresponds to the most highly cross-linked epoxy in our experiments, i.e., the highest strand density point on Fig. 17. He claims that the presence of crazes results from the existence of local regions of low cross-link density. The presence of such a non-homogeneous strand density (at least on the scale of several micrometres) would be apparent in our microdeformation studies as a spatially varying λ in the deformation zones in our thin films. No such large spatial variation in λ was observed. It seems likely that the "crazes" observed by Morgan, which have "fibril" structures much coarser than craze structures in other glassy polymers, are artifacts resulting from debonding of the epoxy from dust particles and formation of voids at other defects in his films.

These observations in thin films cannot be used directly to infer the absence of crazing in highly constrained bulk samples. For example, while polycarbonate does not craze in thin films at room temperature, it will craze in the highly constrained region under a notch after a certain amount of shear deformation has occurred [41–44]. The plastic constraint increases the equivalent stress for further shear deformation to such an extent that crazing becomes possible. While it is impossible to rule out categorically crazing in macroscopic epoxies on this basis, cracks rather than crazes probably form under plastic constraint in the most highly crosslinked systems.

6. Conclusions

The conclusions are as follows.

(1) The plastic deformation that occurs in these epoxies is profoundly influenced by a network of crosslinked and entangled strands.

(2) The high strand densities in epoxies promotes shear deformation over crazing. It is, therefore, unlikely that conventional epoxies craze.

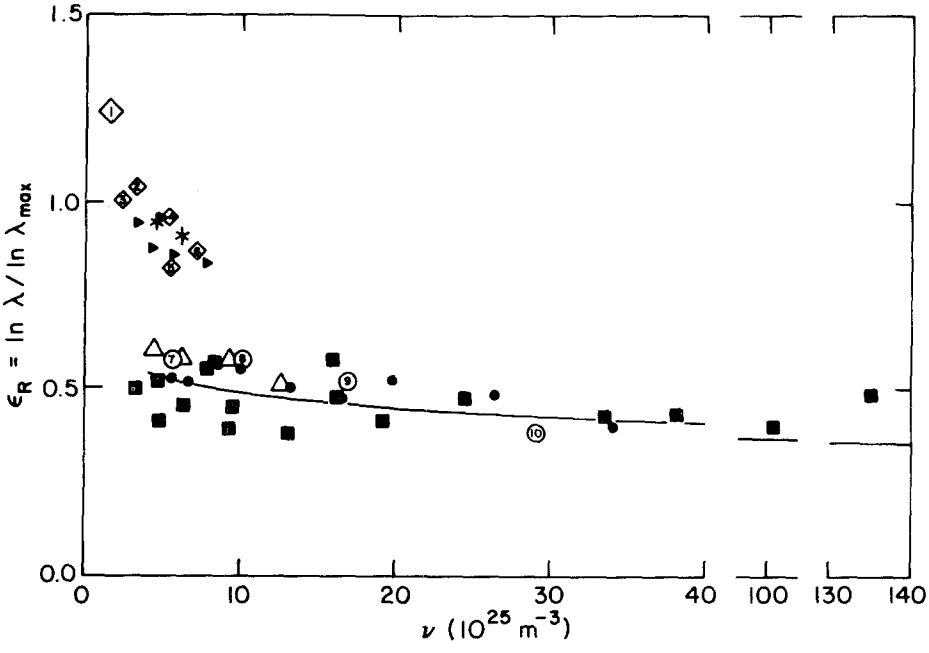

Figure 17 A revised version of Henkee and Kramer's [15] Fig. 8 which now includes the data from this study, shown by the solid squares. Open diamonds and circles, crazes and DZs, respectively, in various uncross-linked homopolymers and copolymers (1-PTBS, 2-PSMLA, 3-PVT, 4-PAMSS, 5-PSAN1, 6-PMMA, 7-PSAN1, 8-PSAN2, 9-PP0, 10-PC; see [15] for a complete key); (*, △, crazes and DZs, respectively, in PS–PPO blends; ▲, ●, crazes and DZs, respectively, in cross-linked PS).

(3) Instead of promoting a transition from shear deformation to crazing by decreasing the network strand density, diluting these epoxies with non-reactive epoxy too short to entangle induced fracture to occur.

(4) The plane stress deformation zones which form in thin films of epoxy are characterized by an extension ratio, λ, which is related to λ_{max}, the maximum extension ratio of a single network strand, by $\lambda - 1 = 0.32\ (\lambda_{max} - 1)$.

Acknowledgements

We acknowledge the support of the Cornell Materials Science Center which is funded by the NSF-DMR-MRL program. We thank Dow Chemical Co (Freeport TX) for providing the various epoxy and phenoxy resins and Steve Hudson for his experimental assistance early in this research.

References

1. S. KUNZ-DOUGLASS, P. W. R. BEAUMONT and M. F. ASHBY, *J. Mater. Sci.* **15** (1980) 1109.
2. R. J. MORGAN and J. E. O'NEAL, *ibid.* **12** (1977) 1966.
3. R. J. MORGAN, J. E. O'NEAL and D. B. MILLER, *ibid.* **14** (1979) 109.
4. R. J. MORGAN, E. T. MONES and W. J. STEELE, *Polymer* **23** (1982) 295.
5. D. C. PHILLIPS, J. M. SCOTT and M. JONES, *J. Mater. Sci.* **13** (1978) 311.
6. R. J. YOUNG, in "Development in Polymer Fracture-1", edited by E. H. Andrews (Applied Science, London, 1979) p. 183.
7. A. J. KINLOCH, *Met. Sci.* **14** (1980) 305.
8. A. J. KINLOCH and J. G. WILLIAMS, *J. Mater. Sci.* **15** (1980) 987.
9. A. J. KINLOCH, S. J. SHAW, D. A. TOD and D. L. HUNSTON, *Polymer* **24** (1983) 1341.
10. A. M. DONALD and E. J. KRAMER, *ibid.* **23** (1982) 1183.
11. *Idem., J. Polym. Sci., Polym. Phys. Edn* **20** (1982) 899.
12. A. M. DONALD and E. J. KRAMER, *Polymer* **23** (1982) 461.
13. A. C.-M. YANG, E. J. KRAMER, C. C. KUO and S. L. PHOENIX, *Macromolecules* **18** (1985) 2020.
14. A. M. DONALD and E. J. KRAMER, *J. Mater. Sci.* **17** (1982) 1871.
15. C. S. HENKEE and E. J. KRAMER, *J. Polym. Sci., Polym. Phys. Edn* **22** (1984) 721.
16. G. POROD, *Monatsh. Chem.* **80** (1949) 251.
17. O. KRATKY and G. POROD, *Rev. Trav. Chim.* **68** (1949) 1106.
18. E. J. KRAMER, *Adv. Polym. Sci.* **52/53** (1983) 1.
19. E. J. KRAMER, *Polym. Eng. Sci.* **24** (1984) 761.
20. L. SCHECHTER, J. WYNSTRA and R. P. KURKJY, *Indian Eng. Chem.* **48** (1956) 94.
21. J. P. BELL, *J. Polym. Sci.* **8** (1970) 417.
22. W. D. BASCOM, R. L. COTTINGTON, R. L. JONES and P. PEYSER, *J. Appl. Polym. Sci.* **19** (1975) 2545.
23. B. D. LAUTERWASSER and E. J. KRAMER, *Phil. Mag.* **39A** (1979) 469.
24. L. SCHECHTER and J. WYNSTRA, *Indian Eng. Chem.* **48** (1956) 86.
25. D. L. PAVIA, G. K. LAMPMAN and G. S. KRIZ, Jr., in "Introduction to Spectroscopy: A Guide for Students of Organic Chemistry", (W. B. Saunders, Philadelphia, 1979) p. 46.
26. H. LEE and K. NEVILLE, in "Handbook of Epoxy Resins", (McGraw-Hill, New York, 1967) Ch. 4.
27. H. R. BROWN, *J. Mater. Sci.* **14** (1979) 237.
28. L. R. G. TRELOAR, in "The Physics of Rubber Elasticity", (Clarendon Press, Oxford, 1975) Ch. 4.
29. J. D. FERRY, in "Viscoelastic Properties of Polymers", (John Wiley, New York, 1980) Ch. 14.
30. P. J. FLORY, in "Principles of Polymer Chemistry", (Cornell University Press, London, 1953) Ch. 9.
31. L. R. G. TRELOAR, in "The Physics of Rubber Elasticity", (Clarendon Press, Oxford, 1975) Ch. 8.
32. R. F. T. STEPTO, in "Developments in Polymerization -3", edited by R. N. Haward (Applied Science, Essex, UK, 1982) Ch. 3.
33. J. L. STANFORD, R. F. T. STEPTO and R. H. STILL, in "Characterization of Highly Crosslinked Polymers", edited by S. S. Labana and R. A. Dickie (American Chemical Society, Washington, DC, 1984) Ch. 1.
34. C. ARENDS, Dow Chemical Co., private communication.
35. J. D. LeMAY, B. J. SWETLIN and F. N. KELLEY, in "Characterization of Highly Crosslinked Polymers", edited by S. S. Labana and R. A. Dickie (American Chemical Society, Washington, DC, 1984) Ch. 10.
36. D. S. DUGDALE, *J. Mech. Sol.* **8** (1960) 100.
37. J. N. GOODIER and F. A. FIELD, Proceedings of the International Conference on Fracture of Solids, edited by D. C. Drucker and J. J. Gilman, Met. Soc. Conferences, Vol. 20 (Interscience, New York, 1963) p. 103.
38. M. D. GLAD, PhD thesis, Cornell University (1986).
39. L. D. LeMAY and F. N. KELLEY, *Adv. Polym. Sci.* **78** (1986) 116.
40. A. J. KINLOCH, C. A. FINCH and S. HASHEMI, *Polym. Comm.* **28** (1987) 322.
41. R. A. W. FRASER and I. M. WARD, *Polymer* **19** (1978) 220.
42. G. L. PITTMAN and I. M. WARD, *ibid.* **20** (1979) 895.
43. N. VERHEULPEN HEYMANS and J. C. BAUWENS, *J. Mater. Sci.* **11** (1976) 1, 7.
44. N. VERHEULPEN HEYMANS, *ibid.* **11** (1976) 1003.

Received 19 September
and accepted 26 September 1989